CETI Session

QUANTITATIVE OBSERVATION OF TRANSMUTATION PRODUCTS OCCURRING IN THIN-FILM COATED MICROSPHERES DURING ELECTROLYSIS

G.H. Miley, G. Narne, M.J. Williams, J.A. Patterson*, J. Nix*, D. Cravens*, and H. Hora‡
Fusion Studies Laboratory, U. of Illinois
103 S. Goodwin Avenue, Urbana, IL 61801-2984
Ph. 217-333-3772, Fax 217-333-2906
E-mail: g-miley@uiuc.edu

ABSTRACT

Several research groups previously identified new elements in electrodes that appeared to be transmutation products (Bockris et al., 1996a; 1996b). However, due to the low concentrations involved, the distinction from possible impurities has been difficult. Now, by using a unique thin-film electrode configuration to isolate the transmutation region, plus measurements based on neutron activation analysis, the authors have achieved, for the first time, a quantitative measure of the yield of transmutation products. Results from a thin-film (500-3000Å) nickel coating on 1-mm microspheres in a packed-bed type cell with 1-molar $LiSO_4$-H_2O electrolyte were reported recently at the Second International Conference on Low-Energy Nuclear Reactions (Miley and Patterson, 1996). Key new results are now presented for thin-film Pd and for multiple Pd/Ni layers. The transmutation products in all cases characteristically divide into four major groups with atomic number Z≅ 6-18; 22-35; 44-54; 75-85. Yields of ~1 mg of key elements were obtained in a cell containing ~1000 microspheres (~½ cc). In several cases over 40 atom % of the metal film consisted of these products after two weeks' operation.

INTRODUCTION

Various nuclear transmutation products generated during electrolytic cell operation, typically employing Pd and heavy or light water with various electrolytes, have previously been reported, e.g., see the proceedings of the First and Second International Conferences on Low Energy Nuclear Reactions (Bockris and Lin, 1996a; Bockris, Miley, and Lin, 1996b). Most of these reports dealt with impurity-level quantities of elements, complicating the distinction from impurities. In sharp contrast, the thin (500-3000Å) films used in present work result in the transmutation of a significant percentage of the metal in the thin-film cathode. That result, combined with Neutron Activation Analysis (NAA) and Secondary Ion Mass Spectrometry (SIMS), provide a quantitative measure of the amounts of the various elements produced.

Over a dozen experiments with various thin-film coatings have been carried out in different cells. Thin-film coatings on 1-mm-diameter plastic microspheres, ranging from 500Å-thick single layers of Pd or Ni to multiple Ni/Pd layers, were used in a flowing packed-bed-type electrolytic cell with a 1-molar Li_2SO_4 light water electrolyte. Nuclear reaction products were obtained in all cases, with several runs resulting in concentrations of over 40 atomic % of the metallic film being Fe, Si, Mg, Cu, Cr, Zn, and Ag. Six key runs listed in Table 1 are presented here. A prior publication by Miley and Patterson, 1996, dealt exclusively with the Ni film (run #8) results, while the present paper adds important results for additional Ni runs, for Pd, and for multiple Pd/Ni layers. (The earlier paper, subsequently referenced as M-P 96, contains more

*Clean Energy Technologies Inc., Dallas, Texas 75240
‡University of New South Wales, Australia

Table 1. Summary of runs

Run ID	Packing*	Run 10.0 Duration (hours)	Excess Power (W)
5	#59 PS/NPNPN	520	~ 2 ± 0.5
7A	C1 PS/PN-E	197	~ 4 ± 0.8
8	#60 PS/N	311	~ 0.1-0.9
11	#63 PS/P	211	~ 0.1-0.9
13	#61 GL/N	293	~ 0.1-0.9
18c	#76 PS/N	358	~ 0.1-0.9

*see Table 2 for microsphere data

details about the experimental technique than could be included in the present space-restricted article. Thus, there are frequent references to it.)

The use of thin-film coatings originates from the "swimming electron layer" (SEL) theory proposed earlier (Hora, Miley, et al., 1993; Miley et al, 1993). It suggests that nuclear reactions are assisted by the high interface electron density in multilayer thin-films with alternating metals possessing large differences in Fermi energy levels. Initial experiments used thin-film Pd/Ti coatings sputtered onto a large stainless steel electrode (Miley, et al., 1994). Those experiments were abruptly terminated when the films separated from the substrate soon after loading and heating occurred. Still, high excess heat (estimated to be kW/cm^3 at the interface regions) was observed for minutes prior to loss of the thin-films. Subsequently, Patterson developed a unique electrode configuration using electrochemical deposition of "thick" (μm) metal coatings on mm diameter cross-linked polymer microspheres for use in a flowing packed-bed-type electrolytic cell. The coatings were found to be quite stable in this configuration, so experiments were undertaken to study reaction products using thin-films (500- to 3000-Å thick) laid down by a special sputtering process.

ELECTROLYTIC CELL DESCRIPTION AND OPERATION

The general configuration of the electrolytic cell is shown in Fig. 1. About 1000 microspheres (~0.5 cm^3 volume) were used in the packed-bed cell. Titanium electrodes were employed in most runs. The preheater allows control of the entering temperature of the electrolyte (1 molar $LiSO_4/H_2O$), with flow rates of ~11 ml/min. Voltages across the bed were held at ~2-3 V, with several mA of current, giving an electrical input power of approximately 0.06 W. Inlet-outlet thermocouples provided a measure of the temperature increase of the flowing electrolyte. Positive, but often very small, increases in temperature across the cell, ranging from 0.1 to 4 °C, were observed in all cases.

Loading of hydrogen into the thin-film is done at low (~25 ^{0}C) temperatures, requiring several hours, as observed by an initial increase in the voltage across the bed, followed by an eventual equilibrium voltage level of +2-3 V. Then the cell inlet temperature is slowly raised (over 4-8 hours) to the maximum allowed with the present plastic cell construction, near

CETI Session

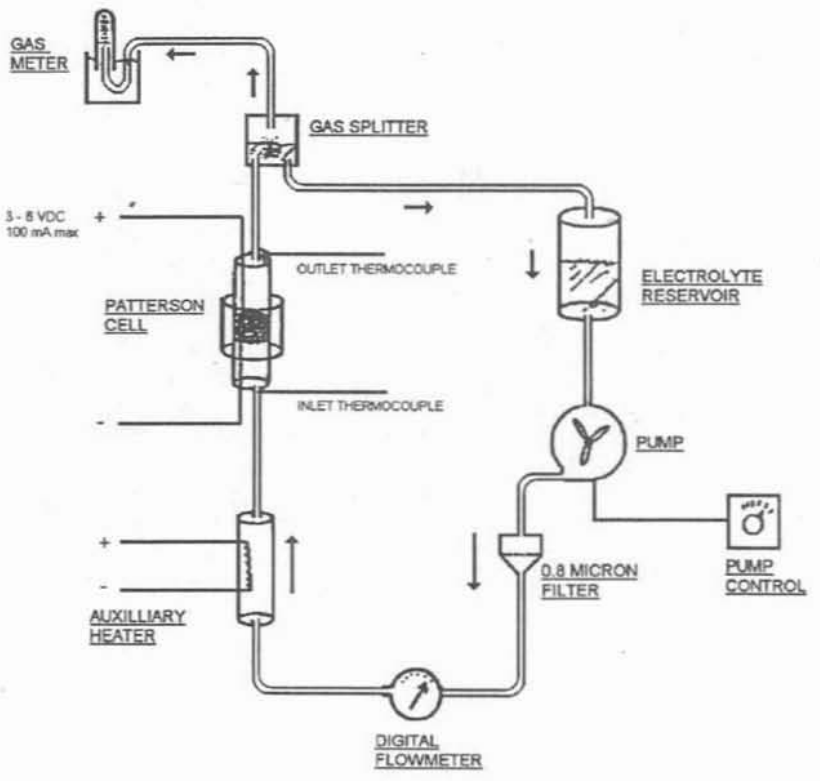

Figure 1. Schematic of flowing cell arrangement

60-70 °C. Run times of several weeks were typical (Table 1). Further details about the construction and operation of this type of cell are given in Patterson, 1996; Cravens, 1995; and Nix, 1996.

Initial runs (#5, 7A, 8) employed a cell with all plastic fittings with the exception of the pressure and flow meters and the pump. Later runs substituted all plastic components ("clean cell" design) except for the electrodes. A filter fitted with 0.8-μm pore size filter paper was employed in the loop (Fig. 1) to collect any fine particles entering the electrolyte, either from film surfaces or from other parts of the system.

THIN-FILM RUNS

Characteristics of the thin-film coated microspheres used are summarized in Table 2. The following nomenclature is adopted: P: palladium, N: nickel, PS: Polystyrene, G: glass. Thus a PS/P/N microsphere has a plastic core with a first coating of palladium and a second coating of nickel. All coatings were sputtered on, unless denoted as -E which used electroplating. The layer masses shown are based on "witness" plate weight measurements during sputtering, hence they are not considered highly accurate compared to element data taken by NAA after a run. Excess power measurements varied from run to run, but the PS/N run was typical for single coatings. It gave a temperature rise of the order of 0.6 °C throughout the run, representing an output of 0.5 ± 0.4 W. Multi-layers gave larger excess power,

approaching 4 W. Calibration corrections due to heat losses and flow-pattern variations limited the measurement accuracy. More precise calorimetry is in use in several laboratories studying excess power from the Patterson Power Cell™, but the present cell design focused on ease of reaction product measurements.

Scanning electron microscope (SEM), photographs of the microspheres confirmed that a very smooth surface was achieved but with a small-scale, rough structure uniformly distributed over it. (see Fig. 2e of M-P 96). Some erosion of small particles and occasional ejection of larger "flakes" from the film occurs during operation as detected by debris collected by the loop filter. Concurrently, various fragile looking bead-like and fiber-like structures are typically visible on the film surface after electrolysis (Fig. 2b of M-P 96). Some structures are perhaps miniature versions of the volcanic-like formations observed on solid electrodes producing transmutations (e.g., Ohmori and Enyo, 1996).

REACTION PRODUCT ANALYSIS METHODS

Reaction product measurements have utilized a combination of NAA, SIMS, Energy Dispersive X-ray (EDX) analysis, and Auger Electron Spectroscopy (AES). NAA can measure total quantities of elements in a sample containing multiple microspheres, while the other techniques are restricted to probing a local area on single microspheres. Due to variations among microspheres arising from location in the packed bed and other effects, this difference in technique is responsible for some of the variations in the results.

Table 2. Data for various thin-film microspheres

PS/N/P/N/P/N (#59; used in Run #5)

Layer	Volume (cc)	Mass of layer (g)	# of atoms
PS (core)	6.22E-04	6.09E-04	-
Ni(300A)	1.06E-07	9.41E-07	9.64E+15
Pd(500A)	1.76E-07	2.11E-06	1.19E+16
Ni(400A)	1.41E-07	1.25E-06	1.29E+16
Pd(800A)	2.82E-07	3.38E-06	1.90E+16
Ni(350A)	1.23E-07	1.10E-06	1.13E+16

PS/P/N-E (#C1; used in Run #7A)

Layer	Volume (cc)	Mass of layer (g)	# of atoms
PS (core)	6.22E-04	6.09E-04	-
Pd(1micron)	3.54E-06	4.24E-05	2.39E+17
Ni(0.5 micron)	1.76E-06	1.57E-05	1.61E+17

PS/N (#60; used in Run #8)

Layer	Volume (cc)	Mass of layer (g)	# of atoms
PS	6.22E-04	6.09E-04	-
Ni(2650A)	9.34E-07	8.31E-06	8.52E+16

PS/P (#63; used in Run #11)

Layer	Volume (cc)	Mass of layer (g)	# of atoms
PS (core)	6.22E-04	6.09E-04	-
Pd(2000A)	7.05E-07	8.46E-06	4.76E+16

G/N (#61; used in Run #13)

Layer	Volume (cc)	Mass of layer (g)	# of atoms
Glass (core)	6.22E-04	1.01E-03	-
Ni(850A)	3.00E-07	2.67E-06	2.73E+16

PS/N (#76; used in Run #18C)

Layer	Volume (cc)	Mass of layer (g)	# of atoms
PS	6.22E-04	6.09E-04	-
Ni(3000A)	1.06E-06	9.41E-06	9.64E+16

Diameter of PS base = 1.06E-01 cm

To distinguish from impurity contributions, both the microspheres and electrolytes were analyzed *before* and *after* the run. Sampling after a run was done by disassembling the cell and removing microspheres from the top (cathode end) layer of the packed bed. (The 1000 microspheres in the bed result in approximately 3-5 layers total). These microspheres were

selected due to accessibility and because the higher electric field in that region should make this layer most reactive. NAA of the microspheres was carried out at the University of Illinois' (UI) TRIGA research reactor (Landsberger, 1996), typically using samples of 10 microspheres. Techniques for short- and long-lived NAA (Parry, 1991) were performed to determine the presence of Ag, Cu, Al, Fe, Cr, Zn, Ni, Co, and V, subsequently termed **"NAA elements."** Typical detection limits were of the order of 2 ppm, with a precision of 2-10%. NAA was also employed to study key isotope ratios (e.g., Cu and Ag) for comparison to natural abundance. Calibration used certified liquid standards from the National Institute of Standards and Technology. Ores containing known quantities of these elements were analyzed simultaneously in all runs for quality control. Further details are described in M-P 96.

The SIMS analysis employed a Cameca IMS 5F unit operating with 8-keV oxygen primary beam in the positive ion mode (Wilson et al., 1989). Scans of key isotopes were made using single microspheres in a low-resolution (2,000 mass resolution) mode at several depths of interest (see Fig. 3a and b of M-P 96). High-resolution (40,000 mass resolution) scans were then done to resolve any interferences involving important isotopes, e.g., see Cu-63 and Ag-107 in Figs. 3c and d of M-P 96. (Elements measured by SIMS, but *not* NAA, are termed **"non-NAA elements"**). Calibration for the SIMS sensitivity was done using the measured concentrations of the nine **NAA elements** as described in M-P 96. SIMS was used to determine isotope ratios except for the Cu and Ag ratios that were determined explicitly by NAA.

The EDX analysis used a Field Emission Electron Microscope (Hitachi S-800) operating in the energy dispersion analysis mode to detect elements with atomic concentrations above 1%. This measurement largely served as added confirmation of NAA measurements (e.g., see Table 2, M-P 96). AES was used in a sputtering mode to perform semi-quantitative depth profiling for the major element species above ~1 atom % (Fig. 5, M-P 96).

RESULTS

ELEMENT AND ISOTOPE CONCENTRATIONS

Results from NAA analyses of the *net* (final minus initial values) yields of high concentration elements in various runs are summarized in Table 3. Element yields as high as several μg/microsphere are obtained, representing roughly a mg of these high-yield elements per cell (1000 microspheres). The corresponding time average reaction rates are of order 10^{16} (atoms/cc film-sec).

To evaluate the concentrations of the **non-NAA elements** present and to obtain isotopic ratios, SIMS and NAA data are combined, e.g., see Table 3 in M-P 96 for run #8. Results for all elements observed in the six runs are shown later in Fig 2, which plots production rates vs. Z. NAA element values are thought to be quite accurate. The **non-NAA element** values are less certain due to uncertainties in the SIMS sensitivity calibration (i.e., "RSF" values) and the restricted location of the measurement on a single microsphere, but the results should still provide a good estimate of ***non-NAA*** isotopes. Further, note that the *isotopic yields* for **NAA elements** should be quite accurate, since the RSF values are constant

for isotopes of a given element, while the total concentrations of these elements are directly from NAA measurements.

ELEMENT DEPTH PROFILES

Data from AES profile measurements on a typical microsphere from PS/N run #8 were presented in Fig. 5 of M-P 96 for the higher concentration elements. Similar results have been obtained for other coatings. Most element profiles distinctly peak in the metal volume or near the metal-core interface, suggesting an internal source rather than diffusion in from the surface. However, the amount of peaking varies among elements and runs, complicating the interpretation of this measurement. Still, the results provide important support for the conclusion that the elements observed did not diffuse in from the surface.

Table 3. Yield for NAA Elements

Yield (micro-grams / microsphere)

Element	Z	Run #5	Run #7A	Run #8	Run #11	Run #13	Run #18C
Ag	47	7.14E-02	1.67E-04	1.60E+00	7.06E-02	2.04E-03	-2.09E-03
Al	13	1.09E-01	2.54E-02	1.39E-02	2.33E-01	-1.78E+00	3.16E-03
Cu	29	3.04E+00	1.24E-01	1.08E+00	2.77E-01	-4.26E-01	3.24E-02
V	23	2.39E-03	2.00E-04	1.05E-03	4.06E-03	-5.71E-03	3.71E-05
Cr	24	4.20E-02	4.46E-03	6.91E-01	6.04E-02	2.34E-02	1.93E-02
Ni	28	H	H	H	3.88E-01	H	H
Fe	26	2.98E-01	3.58E-03	1.78E+00	1.53E-01	5.19E+00	4.56E-02
Zn	30	2.17E+00	1.42E-02	2.99E-01	8.06E-01	3.97E-01	8.24E-02
Co	27	1.46E-03	1.79E-03	1.12E-02	2.18E-03	1.17E-02	4.89E-03

Production Rate (atoms / s - cc of microsphere)

Element	Z	Run #5	Run #7A	Run #8	Run #11	Run #13	Run #18C
Ag	47	3.42E+11	2.11E+09	1.28E+13	8.33E+11	1.74E+10	-1.45E+10
Al	13	2.08E+12	1.28E+12	4.44E+11	1.10E+13	-6.07E+13	8.79E+10
Cu	29	2.47E+13	2.65E+12	1.47E+13	5.55E+12	-6.15E+12	3.82E+11
V	23	2.42E+10	5.35E+09	1.77E+10	1.01E+11	-1.03E+11	5.46E+08
Cr	24	4.17E+11	1.17E+11	1.15E+13	1.48E+12	4.13E+11	2.78E+11
Ni	28	H	H	H	8.41E+12	H	H
Fe	26	2.75E+12	8.73E+10	2.75E+13	3.48E+12	8.53E+13	6.12E+11
Zn	30	1.71E+13	2.97E+11	3.95E+12	1.57E+13	5.57E+12	9.45E+11
Co	27	1.28E+10	4.13E+10	1.64E+11	4.72E+10	1.82E+11	6.22E+10

'H' : Host material

NUCLEAR RADIATION EMISSION

In view of evidence (in Table 3) that products are formed at a significant rate in an operating cell, measurable radiation emission would normally be expected. For example, assuming a rate of about (10^{13} reactions/s-cc ms) x (10^{-3} cc ms) x (10^{3} microspheres) x (1 gamma/reaction) indicates ~10^{13} gammas/sec. To date however, several attempts to measure nuclear radiation emission—neutrons, gammas, or x-rays—during cell operation have not detected any measurable quantities above background (M-P 96). Likewise, several attempts to

measure gamma-ray emission from microspheres removed from the cell after a run also failed to uncover signals above background.

Recently, several sets of PS/N microspheres (run ~4 months earlier) were exposed to high-speed ASA 3000 film (Klema, 1996) for a 4-day period with positive results (Fig. 4 in M-P 96). Unfortunately, these experiments are not very reproducible. A second positive exposure has been obtained, but three additional attempts failed. The technique is under study, and if verified, will demonstrate emission of low-energy beta rays or soft x-rays (estimated to be of the order of 20 keV). Clearly, much more study is needed to fully define possible radiation emission for these cells.

SYSTEMATICS

The yields for both **NAA** and **non-NAA elements** have been converted to element production rates (atoms/cc film-sec) to remove differences arising from variations in the length of runs and are plotted vs. Z in Fig. 2. The rates shown are average values over the run. (Other recent experiments indicate a somewhat faster initial rate and some element-to-element variations. Hence, the use of an average rate for comparisons is somewhat inaccurate, but should provide relative trends.)

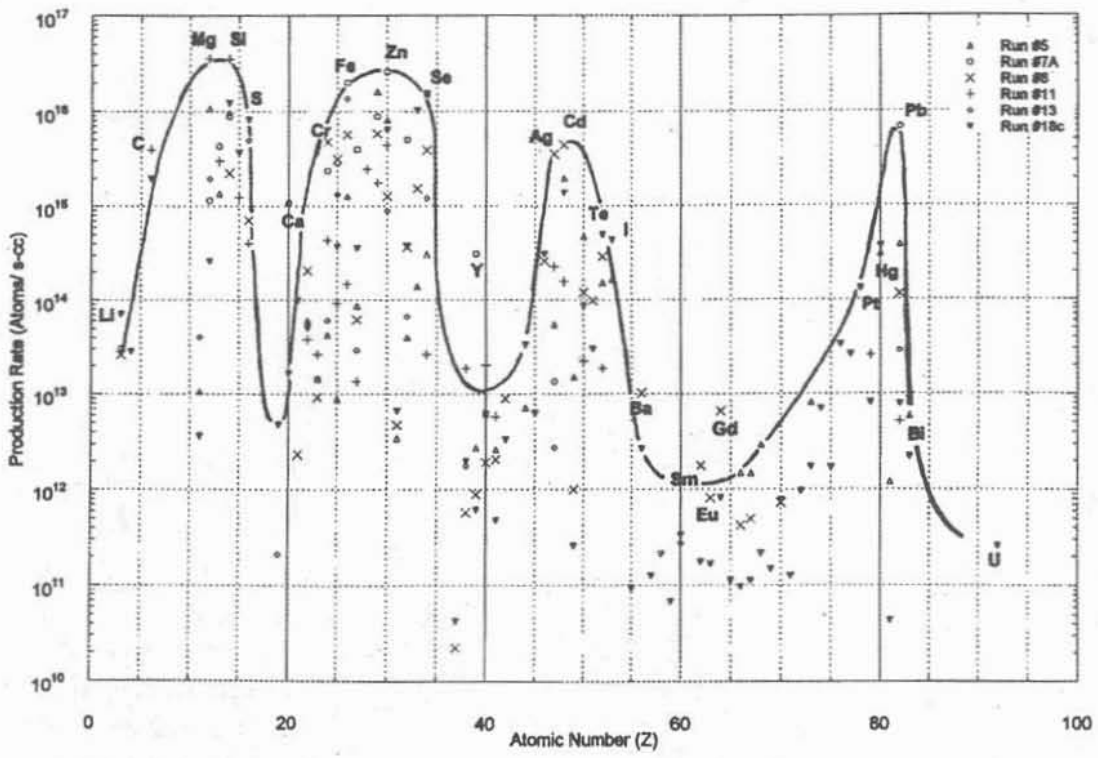

Figure 2. Comparison of atomic production rates for all runs

As indicated in the figure, the composite data of maximum production rates can be enclosed in an envelope with four distinct peaks at Z ~12, 30, 48, and 82. The largest production rates (hence, yields) lay in bands around each peak. This striking result has a close resemblance to the well known two-peak yield curve for neutron-induced fission of uranium (Katcoff, 1960). For that case, the peaks are associated with light and heavy fission products arising from the break-up (fission) of the neutron-uranium compound nucleus. Thus, one interpretation for the present result is that the peaks of Fig. 2 also represent the fission of compound nuclei, created in this case by proton-metal reactions. The startling fact that elements in the higher Z peaks lay above the host metals (Ni or Pd) would then require multi-atom fusion to form a compound nucleus capable of fissioning into these high-Z products. This view of the reaction mechanism is discussed in more detail later.

Comparison of the data for the individual runs in Fig. 2 provides further important insight. Runs #8 and #18c, both of which used 650-Å Ni film on a plastic core, are shown in Figs. 3a and b for clarity. However, they were done four months apart in different laboratories (U of Illinois and CETI, Florida, respectively) with different cells. The recent CETI run (#18c) used an ultra-pure cell (the only metal parts were the titanium electrodes) and the highest purity electrolyte (99.996% $LiSO_4$) with an additional pre-run with "sacrificial microspheres" for added purification. With these added precautions, impurity levels in the electrolyte in run #18c were reduced by a factor of 4-5 compared to the earlier run. But surprisingly, more reaction products were observed in #18c than in #8 (64 elements vs. 37 respectively), while the absolute rates for high-yield elements and the four-peak characteristic remains fairly similar. In that sense, the reproducibility of the experiment appears quite good. In the sense that products with characteristic four-peak behavior have been obtained in the dozen-plus experiments attempted to date, the reproducibility is excellent. This is in sharp contrast to the widely-recognized lack of reproducibility in conventional "cold fusion" experiments aimed at heat production. However, more experience with the thin-film concept by other independent researchers is needed before a final decision about reproducibility can be reached.

Run #13 (G/N) in Fig. 3c employed Ni on a glass (vs. plastic) core. As seen from the figure, this resulted in a distinct decrease in products in the third and fourth groups (higher Z) and slightly reduced the yields in the first and second groups. Concurrently, this run was unique in showing, cf Table 3, a decrease in Al, Cu and V levels. These results suggest that the core material plays a role in the mechanism. However, the basis for this effect requires more study—it could be attributed to differences in the swimming electron layer at the core-metal interface or to the interaction of the core material with the host matrix. These differences may be responsible for failure by other workers to obtain excess heat with independent G/P/N microsphere experiments (Schaffer, 1996).

The PS/P (palladium) core experiments (Fig. 4) also show a "four-peak" behavior, but, unlike the corresponding Ni runs, the amplitudes of the peaks decrease progressively in going to high-Z. Also, there appears to be a void of products between the third and fourth peaks. These results allow an interesting comparison with the solid Pd electrode (D_2O/Li_2CO_3 electrolyte) study by Mizuno et al., 1996. In that experiment, the products with non-natural isotopic abundance were observed in a thin region about 1 mm beneath the electrode source.

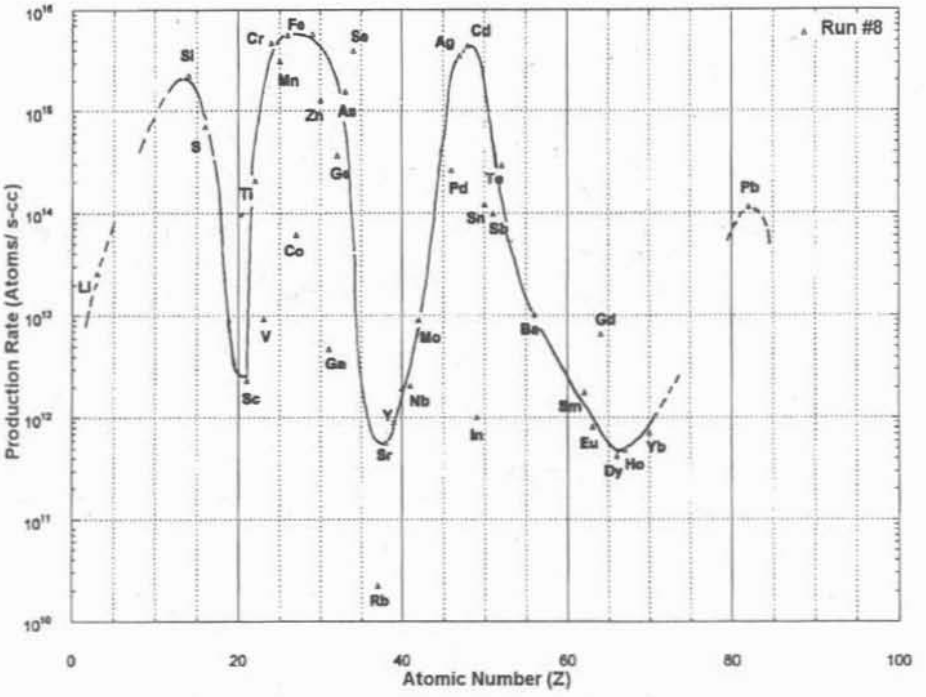

Figure 3a. Initial PS/N run done 3/96

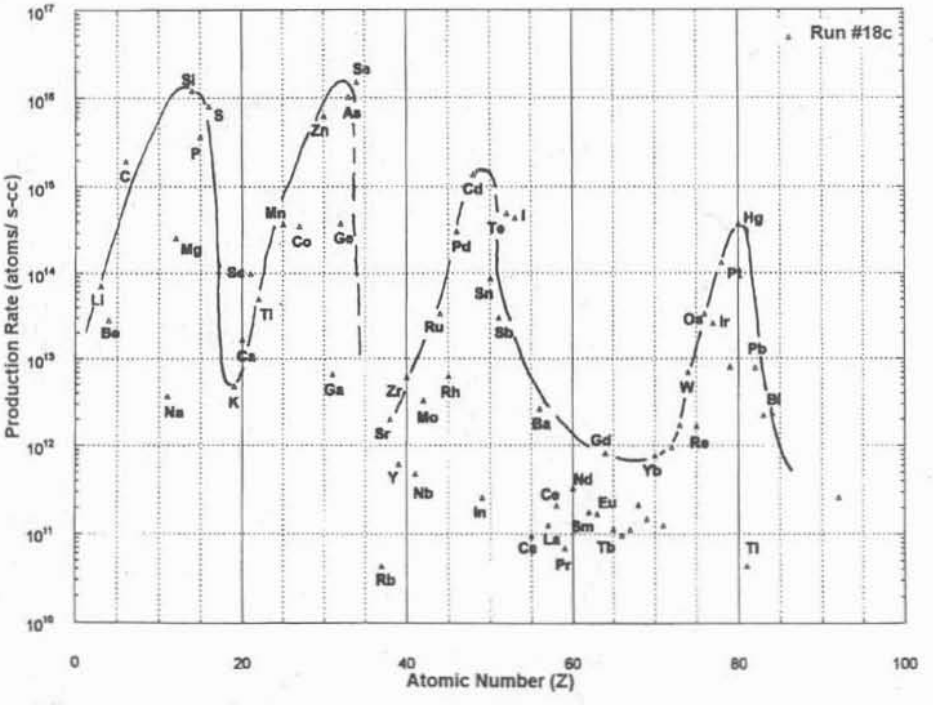

Figure 3b. Run #18c with PS/N microspheres - a duplication of run #8 using "ultra" clean cell conditions

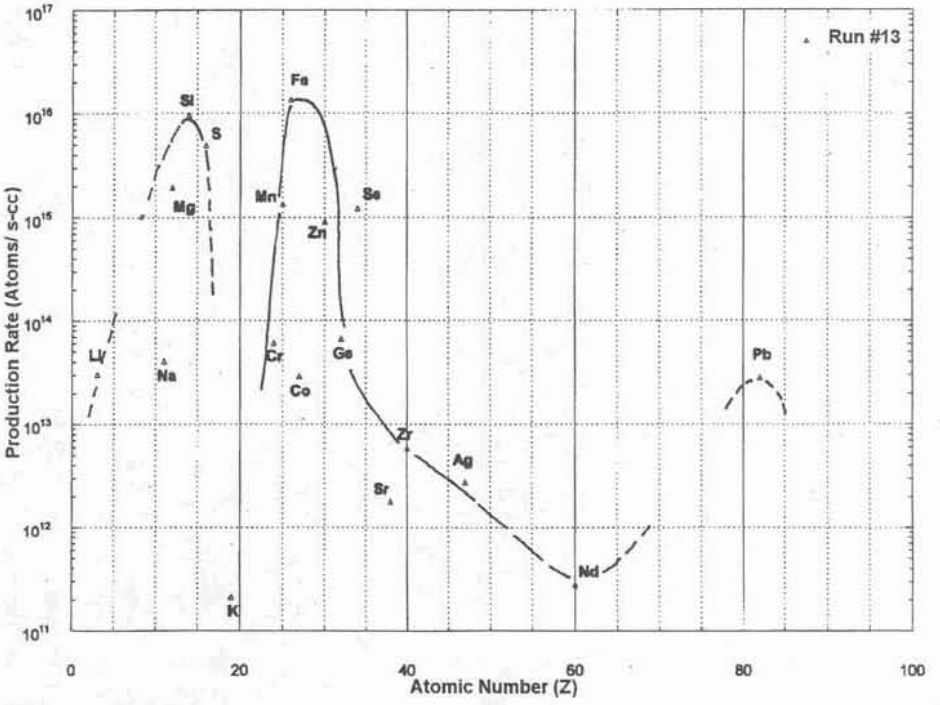

Figure 3c. Run #13 with GL/N (glass core) microspheres - compare with Figs. 3a and b for Ni on plastic cores

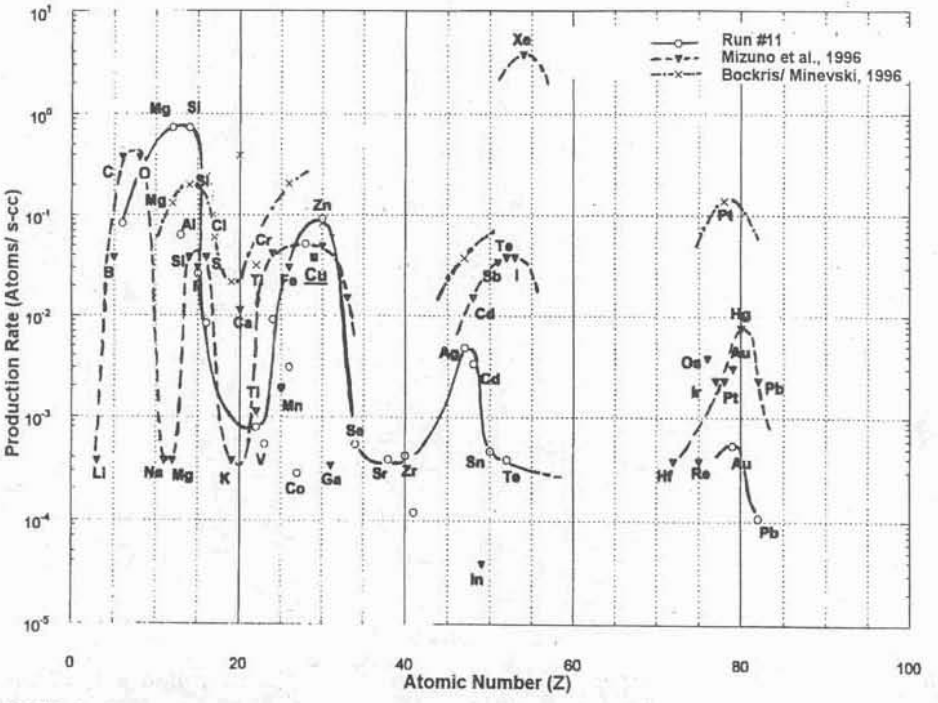

Figure 4. PS/P (palladium Run #11) and related to data for solid Pd D_2O electrolytic cell by Mizuno et al., 1996 and Bockris/Minevski, 1996 (both normalized to Cu data from Run #11)

Related results argued to be "too deep" to be impurities reported earlier by Bockris and Minevski, 1996, are also included in the figure. In contrast to present experiments, absolute production rates were not obtained in either of the solid electrode experiments; thus for comparison, yield data are normalized in Fig. 4 to the present Cu production rate. Again, the 4-peak structure is observed for both sets of data. A striking difference is observed in the third peak products where larger production rates, especially for Xe, are reported by Mizuno et al. and in the fourth peak where Mizuno reports a wider variety of elements and a high Pt rate is reported by Bockris/Minevski. A possible explanation for differences in gaseous products such as Xe is that in the present experiments gases rapidly diffuse out of the thin-films, preventing detection. In general, however, the similarity of results from independent experiments using radically different electrode design and electrolytes, suggests that the four-peak product curve is a general characteristic of this phenomenon. While amplitudes (yields) change with cell characteristics, the general shape of the curve remains intact. (Other product data appears to have this shape, but the results are less definite, e.g., see Karabut et al, 1991; Celani, et al, 1996; Ohmori and Enyo, 1996).

The two multi-layer runs (#5 and #7a included in Fig. 2) follow the same general trend as the single-layer runs. Physically #7a differed from #5 by having fewer layers (two vs. five), and used much thicker (~1μm vs. 300-500Å) layers made by electroplating. Run #5 in particular shows a rich array of products (similar to the PS/N run #18c) whereas #7a has few products in the region of the third and fourth yield peaks. Interestingly, consistent with SEL theory, the multiple layers also produced the most excess heat of all six runs; see Table 1. The depth probe scans for the multi-layer runs confirm that the product concentrations decrease with distance from the Pd/N interface(s), suggesting that the reaction occurs preferential there, in agreement with SEL theory.

Added runs are in progress to clarify the issue of heat production and its tie to the various yield curves. A general view, however, is that heavy elements generally involve low or negative Q-values (endothermic) reaction whereas light elements involve positive Q-values; the net energy produced, i.e., excess heat, involves the difference (or "net") of ±Q-values. This postulation could explain why reaction products apparently can occur without a large heat production. Since the net balance involves differences in large numbers, small changes can drastically affect the ability to produce excess heat, perhaps explaining why excess heat experiments appear to be so irreproducible.

Isotope Shifts

The change in % abundance of the various isotopes, as measured by SIMS, relative to natural abundance is summarized in Fig. 5 (changes <2% suppressed for clarity). From this result it is seen that a majority of the isotopes observed have measurable shifts. The larger values, marked with element symbols, are typically low-yield elements, although some high-yield elements have significant shifts. A pattern is not obvious, however, and the problem is further complicated by variations of the isotope ratios with depth into the film and location on the microspheres. Still, despite these variations, the many shifts observed add further strong

support to the conclusion that the elements observed are not impurities, which would be expected to exhibit natural abundances.

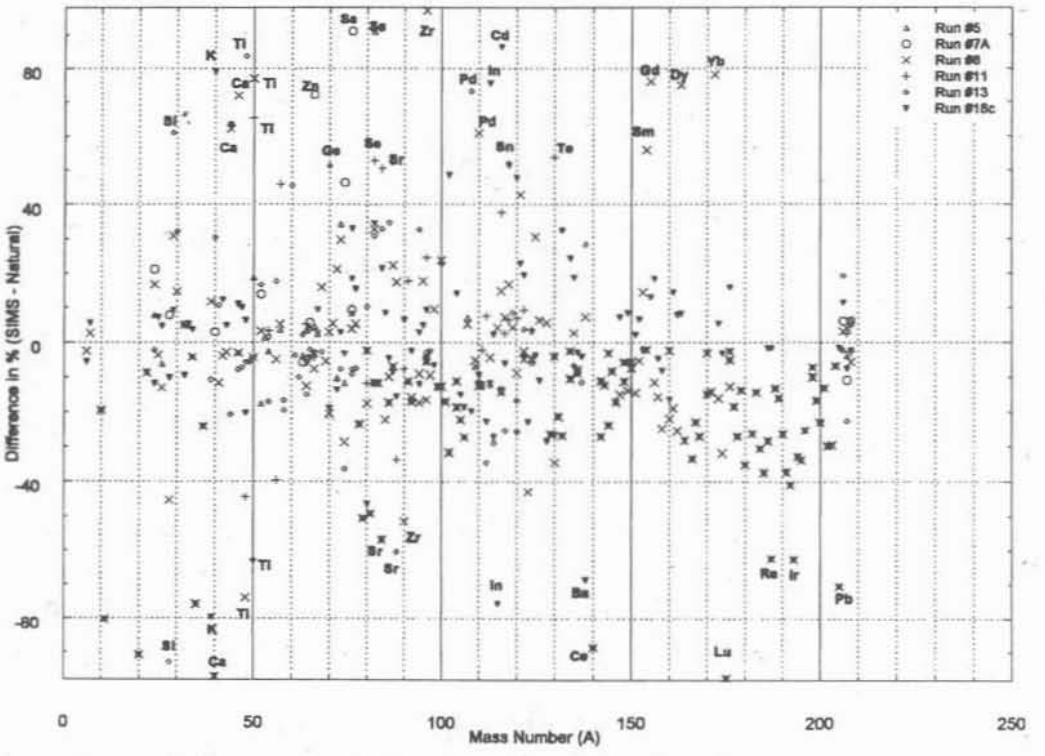

Figure 5. Summary of isotope shifts for all runs as measured by SIMS

Since Cu and Ag are key heavy elements, further confirmation for their shifts, obtained from NAA, is in progress. First results for Cu for run #8 with Pd/N gave Cu-63: +3.6 ±1.6%; Cu-65: -8.1 ±3.6% while corresponding SIMS values (Fig. 5) are Cu-63: +0.8%, Cu-65: -0.8%. While there are differences in magnitude, the positive and negative trends agree. The differences are thought to be due to the localized nature of the SIMS values compared to NAA results, which represent an average over the 10 microsphere samples employed.

In summary, despite variations in the individual runs, the data strongly supports the conclusion that significant deviations from natural abundance occurred.

IMPURITY ISSUES

The use of thin-films introduces a potential impurity problem in reaction product studies due to the small volume occupied by the film vs. the large volume of the electrolyte. Consequently, NAA measurements of the nine **"NAA elements"** were made on samples of microspheres, electrolytes and filter paper both before and after a run. (SIMS meaurements were also done on microspheres before and after runs.) Quantities of these **NAA elements** found prior to the run were consistently <10% of that found after the run (except for Al, which was initially higher); see Table 4a of M-P 96. Analysis of other cell components, i.e., the electrode and plastic components, did not uncover significant impurity concentrations of the

NAA elements. Other tests included a "null" run with electrically conductive sulfonated plastic beads used to simulate metal-coated beads (M-P 96). Substitution of platinum for the titanium anode did not affect results. Various runs presented here used three entirely different cells. The first PS/Ni run employed some metal fittings in the loop which were thereafter substituted out

in favor of plastic. Run #13 used an entirely new all plastic cell (the electrodes being the only metal components) with an electrolyte that was first run with "sacrificial" PS/N microspheres for a week (to collect impurities on the microspheres) before new microspheres were loaded and used for the actual run.

No impurity concentrations near the magnitude of the **NAA elements** found in the film following the runs were identified with these exhaustive tests, strongly supporting the conclusion that these elements were produced by nuclear transmutations. Results for the other **non-NAA elements** measured by the SIMS are less definite since their initial concentrations were measured in the microsphere, but not in the electrolyte, leaving impurity issues open. Still, there are other evidences (e.g., isotopic shifts from natural abundance) that most of these elements too, cannot be attributed to impurities.

In conclusion, the finding that the masses of the key isotopes following a run are large compared to possible sources of such isotopes from loop components, the negative results from simulation runs without Ni or Pd films, the observation of isotope shifts from natural abundance, and the observation that the isotopes vary with film material all combine to provide very strong evidence that the products reported are not caused by impurities.

REACTION MECHANISM CONSIDERATIONS

A nuclear explanation for the products requires an entirely new theory for chemically-assisted reactions in solids. Here it is possible only to point out some features that should be considered in such a theory. In the present case, the SEL theory cited earlier offers a possible explanation for overcoming the Coulombic barrier between ions in a multilayer thin-film electrode. However, this theory does not explain what reactions occur once barrier penetration is achieved. In view of the large yields obtained, the reactants must involve some of the key species present, namely: Li, S, or O from the electrolyte; C or H from the plastic microsphere core; Ni or Pd from the thin-films (cathode); and H, i.e., protons (p) from the light water. The following discussion assumes that the main reactions involve p-Ni or p-Pd interactions.

The concept that excess heat from electrolytic cells originates from reactions involving the electrode material is not new. Ragheb and Miley, 1989, originally proposed that in a Pd-D_2O cells, Oppenheimer-Phillips-type neutron-stripping reactions between the D and Pd might explain early observations. Later, Miley (Appendix B in Hoffman, 1995) summarized the status of such theories, and introduced a table of possible p-Pd reactions (including examples of fission-type reactions). The present results with high-Z products add a new dimension to these thoughts, however.

A key feature observed in Fig. 2 that must be accounted for is the four-peak curve, where the two higher Z peaks include elements significantly heavier than the host metal (Ni or

Pd). These heavy elements infer an endothermic reaction (-Q-value), which in turn suggests energy transfer to the reactants must occur to drive the reaction. (This is analogous to driving -Q-value reactions by colliding high-energy reactants using accelerated beams.) Consequently, the model must contain a mechanism for energy storage/transfer to reactions involved in high-Z element production.

The observed excess power and the estimated reaction rates for element production also pose a dilemma. Based on Table 3, present cells undergo about 10^{13} reactions/5-cm^3 ms. Thus, the single-layer runs with excess power of about 0.5 W correspond to an average energy release of ~6 x 10^{-2} MeV/atom reacting in the 1000-microsphere cell. That is considerably lower than the energy typically obtained from exothermic nuclear reactions expected in p-metal interactions (Miley, in Hoffman, 1995). This contradiction can possibly be explained if the excess energy released is reduced by endothermic reactions that "absorb" energy in the formation of heavier elements. As noted earlier, the view that excess energy involves a delicate balance between + and -Q reactions could partly explain why excess heat type experiments are often not reproducible. Conversely, this implies that transmutation product may be a more reproducible signal of reactions than heat, since products can be obtained, according to this view, even in a cell not producing significant excess heat.

The lack of intense high-energy radiation is another key characteristic that must be explained. This appears to be associated with energy transfer to the lattice via a coherent mechanism and "slow" reactions that allow relaxation to stable states, e.g., see Kucherov, 1996; Hagelstein, 1996.

A postulated reaction model, RIFEX (Reaction In a Film-Excited CompleX), is under development to satisfy these key characteristics. A major feature of RIFEX is that protons (p) interacting with the host Ni produce a relatively long-lived atom-p complex with excitation energies of orders of several MeV. This allows the production of heavy compound nuclei that subsequently fission. This model will be presented in detail in a future publication.

CONCLUSION

The use of thin-film electrodes has been shown to provide a unique and important method to study nuclear transmutations in electrolytic cells. By localizing the reaction, these films, combined with NAA and SIMS analyses, allow, for the first time, quantitative measurements of yields. As demonstrated by duplicate nickel-film runs, good reproducibility appears possible. However, as the authors stressed earlier (M-P 96), others are invited (and strongly encouraged) to investigate this new technique to provide full proof of reproducibility.

The most striking and unexpected result is the characteristic four-peak yield curve that appeared in all runs, but with various differences in numbers of products in various regions around the peaks. This curve, containing high-Z materials in the higher peaks, inescapably implies that multi-body reactions must occur. Since there is still debate about how deuteron ions can overcome the Coulombic barrier in "conventional" experiments, the implication that multi-body high-Z reactions occur greatly stretches the understanding of this phenomena. Various collective effects appear to be involved, although the initiation could still proceed via

swimming electron layer screening at interfaces. Theoretical studies are urgently needed to shed light on this amazing phenomenon, assuming that experimental reproducibility is confirmed by others.

REFERENCES

Bockris, J.O'M and G.H. Lin (organizers), 1996a. Proceedings of the First International Conference on Low Energy Nuclear Reactions Conference, *J. New Energy,* in press.

Bockris, J.O'M, G.H. Miley, and G.H. Lin (organizers), 1996b. Proceedings of the Second International Conference on Low Energy Nuclear Reactions Conference, *J. New Energy,* 1, 1, 111-118.

Bockris, J.O'M and Z. Minevski, 1996, "Two Zones of 'Impurities' Observed After Prolonged Electrolysis on Palladium," *Infinite Energy,* vol. 1, no. 5 & 6, 67-69.

Celani, F., 1996, Istituto Nazionale di Fisica Nucleare, Italy, personal communication.

Cravens, D., 1995, "Flowing Electrolyte Calorimetry," *Proc. 5th Intern. Conf. on Cold Fusion*, Valbonne, France, IMRA Europe, 79-86.

Hagelstein, P., 1996, "Lattice Induced Reactions," Abst. P-056, ICCF-6, Hokkaido, Japan

Hora, H., J. C. Kelly, J. U. Patel, M. A. Prelas, G. H. Miley, and J. W. Tompkins, 1993, "Screening in Cold Fusion Derived from D-D Reactions," *Physics Letters A*, 175, 138-143.

Karabut, A.B., Ya.R. Kucherov, and I.B. Savvatimova, 1991, "The Investigation of Deuterium Nuclei Fusion at Glow Discharge Cathode," *Fusion Technol., 20,* 924.

Karabut, A.B., Ya.R. Kucherov, and I.B. Savvatimova, 1992, "Nuclear Product Ratio for Glow Discharge in Deuterium," *Physics Letters A*, 170, 265.

Katcoff, S, 1960, "Fission-Product Yields from Neutron-Induced Fission," *Nucleonics,* 18, No. 11, 201.

Klema, E., 1996, Tufts University, Medford, MA. Private communication.

Kucherov, Y., 1996, "Slow Nuclear Excitation Model," Abs. P-006, ICCF-6, Hokkaido, Japan.

Landsberger, S., 1996, Dept. of NucE., U. of IL, Urbana, IL, private communication.

Schaffer, M., 1996, General Atomics Corp., San Diego, CA, personal communication.

Miley, G.H., M. Ragheb, and H. Hora, 1989, "Comments about Nuclear Reaction Products from Cold Fusion," Proceedings, NSF/EPRI Workshop, Washington DC, 16-18 October 1989.

Miley, G.H., J.U. Patel, J. Javedani, H. Hora, J.C. Kelly, and J. Tompkins, 1993, "Multilayer Thin-film Electrodes for Cold Fusion," *Proc. ICCF-3*, Frontiers In Science Series No. 4, ed. H. Ikegami, Universal Academy Press 659-663.

Miley, G.H., 1995; in Hoffman, N., *A Dialogue on Chemically Induced Nuclear Effects: A Guide for the Perplexed about Cold Fusion*, La Grange Park, IL, The American Nuclear Society, Appendix C, 146-154.

Miley, G.H., H. Hora, E.G., Batyrbekov, R.L. Zich, 1994, "Electrolytic Cell with Multilayer Thin-Film Electrodes," *Trans. Fusion Technol., 26*, 4T, Part 2, 313-320.

Miley, G.H. and J.A. Patterson, 1996. "Nuclear Transmutations in Thin-Film Nickel Coatings Undergoing Electrolysis," Proceedings of the 2nd International Conference on Low Energy Nuclear Reactions, Texas A & M, College Station Texas, September 13-14. (in press, J. New Energy). ***[Referred to as M-P 96]***

Mizuno, T., T. Ohmori, and M. Enyo, 1996, "Changes of Isotope Distribution Deposited on Palladium Induced by Electrochemical Reaction," *J. New Energy*, 1,1, 23-27.

Nix, J., 1996, "Revised Protocol for Patterson Cell Assembly and Operation," Memorandum, Clean Energy Technologies, Inc., 3 May 1996.

Ohmori, T., and M. Enyo, 1996, "Iron Formation in Gold and Palladium Cathodes", *J. New Energy*, 1, 1, 15-22.

Parry, S.J., 1991, *Activation Spectrometry in Chemical Analysis*, in *Chemical Analysis*, ed. J.D. Winefordner, Vol. 119, John Wiley and Sons, NY.

Patterson, J.A., 1996, "System for Electrolysis," U.S. Patent #5,494,559, 27 Feb. 1996.

Wilson, R.G., F.A. Stevie, C.W. Magee, 1989, *Secondary Ion Mass Spectrometry: A Practical Handbook for Depth Profiling and Bulk Impurity Analysis*, John Wiley & Sons, N.Y.

ACKNOWLEDGMENTS

This work was supported by a grant from CETI. S. Landsberger (UI) carried out the NAA analysis. J. Reding (CETI) coordinated the UI and CETI efforts. R. Twardock (UI), and E. Klema (Tufts U) carried out radiation measurements on microspheres. Valuable comments by M. McKubre (SRI) and P. Hagelstein (MIT) are also gratefully acknowledged.